Exchange-Correlation Catastrophe in Cu-Au: a Challenge for Semilocal Density Functional Approximations

Li-Yun Tian,[1,2] Henrik Levämäki,[3,4] Matti Ropo,[5,6] Kalevi Kokko,[3,4] Ágnes Nagy,[7] and Levente Vitos[1,8,9]
[1]*Applied Materials Physics, Department of Materials Science and Engineering, Royal Institute of Technology, Stockholm SE-100 44, Sweden*
[2]*Key Laboratory of Materials Modification by Laser, Ion, and Electron Beams of Ministry of Education, Dalian University of Technology, Dalian 116024, China*
[3]*Department of Physics and Astronomy, University of Turku, FI-20014 Turku, Finland*
[4]*Turku University Centre for Materials and Surfaces (MatSurf), Turku, Finland*
[5]*Tampere University of Technology, Department of Physics, FI-33101 Tampere, Finland*
[6]*COMP/Department of Applied Physics, Aalto University School of Science, PO Box 11100, FI-00076 Aalto, Finland*
[7]*Department of Theoretical Physics, University of Debrecen, H-4010 Debrecen, Hungary*
[8]*Department of Physics and Astronomy, Division of Materials Theory, Uppsala University, Box 516, SE-75121, Uppsala, Sweden*
[9]*Research Institute for Solid State Physics and Optics, Wigner Research Center for Physics, Budapest H-1525, P.O. Box 49, Hungary*
(Dated: May 27, 2016)

Semilocal density functional approximations occupy the second rung of the Jacob's ladder model and are thus expected to have certain limits to their applicability. Recently, it has been hypothesized that the formation energy, being one of the key quantities in alloy theory, would be beyond the grasp of semilocal Density Functional Theory (DFT). Here we explore the physics of semilocal DFT formation energies and shed light on the connection between the accuracy of the formation energy and the ability of a semilocal approximation to produce accurate lattice constants. We demonstrate that semilocal functionals designed to perform well for alloy constituents can concomitantly solve the problem of alloy formation energies.

PACS numbers: 71.15.Mb, 71.20.Be, 64.30.Ef, 71.15.-m

Density Functional Theory (DFT) with its various practical approximate forms has come to have a deep impact on many different fields of science. The local and semilocal exchange-correlation (XC) schemes, such as the Local Density Approximation (LDA) and the Generalized Gradient Approximation (GGA) [1], are two of the most important levels (first and second rungs of the Jacob's ladder model [2]) on the DFT XC approximation gamut. Recently, there has also been important developments in meta-GGAs (third rung of the Jacob's ladder), where the functional also includes dependence on the kinetic energy density. Empirical meta-GGAs, e.g. the M06 family [3–5], and recent nonempirical meta-GGAs, such as MGGA-MS2 [6] and SCAN [7], can lead to significant improvements in both structure and energetics [8].

The computational efficiency of the first three rungs of the Jacob's ladder is superior compared to most of the more sophisticated approaches. Naturally, for this reason semilocal XC approximations are in many instances preferred, especially when large amounts of individual calculations are involved. Therefore, it is vitally important to establish a clear picture of the limits and capabilities of semilocal approximations.

In a recent Letter by Zhang *et al.* [9], it was surmised that conventional semilocal DFT simply falls short of being able to accurately predict key properties in alloy theory, such as the formation energy. One of the most spectacular failures happens with the well-known Cu-Au system showing a series of intermetallic compounds. Zhang *et al.* found that the experimental formation energies of these intermetallics are far smaller in magnitude than their (semi)local DFT counterparts and concluded that nonlocal exchange interaction schemes, such as the Heyd-Scuseria-Ernzerhof (HSE) hybrid functional [10, 11], are necessary in order to mitigate the delocalization error of standard approximations and to increase the accuracy of the theoretical predictions. This finding has raised strong doubts concerning the scope of (semi)local DFT and in particular the applicability of LDA or Perdew-Burke-Ernzerhof (PBE) [12] GGA to Cu-Au and similar important members of the highly versatile class of metallic alloys.

In this Letter, we adopt an energy functional perspective and investigate whether an appropriate GGA functional better suited for the particular alloy system would be able to eliminate the observed discrepancies in the formation energies. We identify the source of the GGA DFT formation energy problem as being similar in nature to the one causing the inaccurate description of the equation of states. Specifically, in order to obtain accurate GGA formation energies for metallic alloys, the GGA XC functional needs to be capable of consistently describing the ground states for all alloy components simultaneously. Presently, on the GGA level [12–14], only XC functionals based on the subsystem functional ap-

proach (SFA) [15, 16] are able to fulfill this requirement.

The Quasi-Non-uniform exchange-correlation Approximation (QNA) was developed for solids and alloys [17, 18] and it utilizes SFA by treating each element in the periodic table as an individual subsystem, providing each of them with an "optimal" subsystem functional. The "optimal" functionals in turn are established by using information available for pure elements in their ground state structure. Here, we compare the QNA level theoretical predictions for the lattice constants and formation energies of the Cu-Au system to those obtained using the standard PBE and SCAN meta-GGA. In contrast to PBE, QNA is found to give perfect equilibrium volumes and bring the formation energies very close to the experimental and HSE results reported by Zhang *et al.* [9]. Similar trends can be observed in our SCAN results. We postulate that in terms of accurate equation of states and formation energies, a well chosen semilocal functional can achieve accuracy comparable to the cumbersome non-local functionals. We demonstrate the robustness of our posit on a variety of other binary compounds: Cu-Pd, Cu-Ag, Cu-Pt, Ag-Pd, Ag-Au, and Ni-Al. In each of these cases, the performance of QNA-SFA is very promising.

For all configurations, the electronic structure calculations were performed within the DFT-LDA framework, using the exact muffin-tin orbitals method [19–22] for solving the Kohn-Sham equations. The total energies were obtained within the full charge density technique [20], and for the energy functional we adopted the PBE and QNA schemes. The energy functionals were evaluated non-selfconsistently using converged LDA densities. This perturbative approach introduces negligible error in the total energy compared to full PBE/QNA calculations [23–25]. Numerical parameters were chosen to provide well converged physical quantities. The Cu-Au system was described considering the face centered cubic (fcc) lattice for Cu and Au, the $L1_2$ structure for Cu_3Au and $CuAu_3$, and a tetragonally distorted $L1_0$ structure for CuAu [26–28]. The c/a for the latter lattice was set to 0.915, which is consistent with the reported values [29, 30]. The following QNA parameters were used: Cu, Pd, Ag, Au (Ref. [18]), Al ($\mu = 0.115$, $\beta = \beta_{\mathrm{PBEsol}}$), Ni ($\mu = 0.115$, $\beta = \beta_{\mathrm{PBE}}$), and Pt ($\mu = \mu_{\mathrm{LDA}}$, $\beta = \beta_{\mathrm{LDA}}$).

In the upper panel of Figure 1, we compare the present lattice constants for Cu, Cu_3Au, CuAu, $CuAu_3$ and Au with the previous theoretical results obtained using the Linear Muffin-Tin Orbitals (LMTO) and the Augmented Spherical Wave (ASW) methods (both LDA level) [31, 32], the Projector Augmented Wave (PAW) method (PBE level) [33], and the available experimental data [30, 37, 38]. As expected, the lattice constants obtained using QNA and SCAN are in good agreement with the experimental values over the whole concentration range. At the same time, the equilibrium volumes are strongly overestimated by PBE, especially for Au-rich

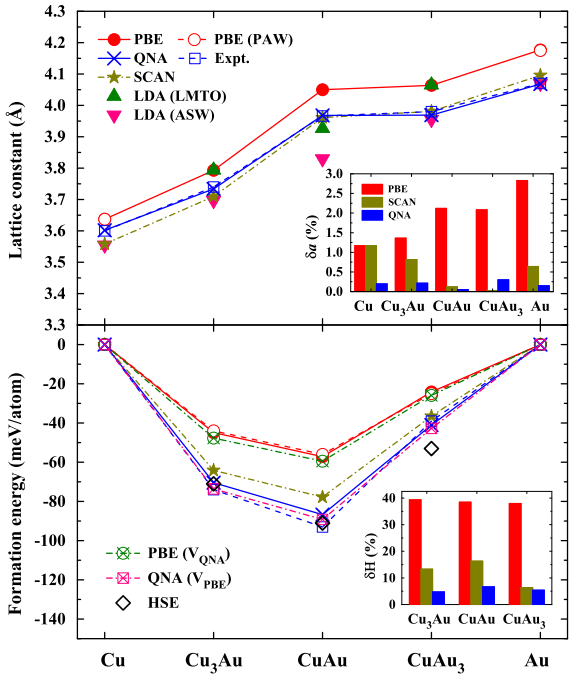

FIG. 1. (Color online) Comparison of the present lattice constants (upper panel) and formation energies (lower panel) for the Cu-Au system calculated at PBE, QNA, and SCAN levels to the previous theoretical values (denoted by PAW, LMTO, ASW, and HSE) [9, 31, 32] and the experimental data [9]. The upper legend applies to both panels. The insets show the errors of the present PBE, QNA, and SCAN lattice parameters (δa) and formation energies (δH) relative to the experimental data.

alloys, which is a known shortcoming of this approximation [23].

The present formation energies of the Cu-Au system are compared to the experimental data and previous HSE results [9] in the lower panel of Figure 1. The PBE formation energies are nearly a factor of two too small in magnitude, a fact which has been noticed by Zhang *et al.* [9] and Ozoliņš *et al.* [39]. SCAN gives a noticeable improvement over PBE. Interestingly, QNA produces formation energies that agree very well with the experimental data. One might naïvely assume that the outstanding performance of QNA is simply due to the so called "volume effect" meaning that if PBE calculations were repeated using QNA volumes, the so-obtained PBE formation energies would be more accurate. This, however, is not the case: in the lower panel of Fig. 1 we show results obtained by repeating the PBE calculations using the QNA volumes (V_{QNA}). The corresponding formation energies are in fact very close to the full PBE results. On the other hand, repeating the QNA calculations using the PBE volumes (V_{PBE}) does not destroy the excellent

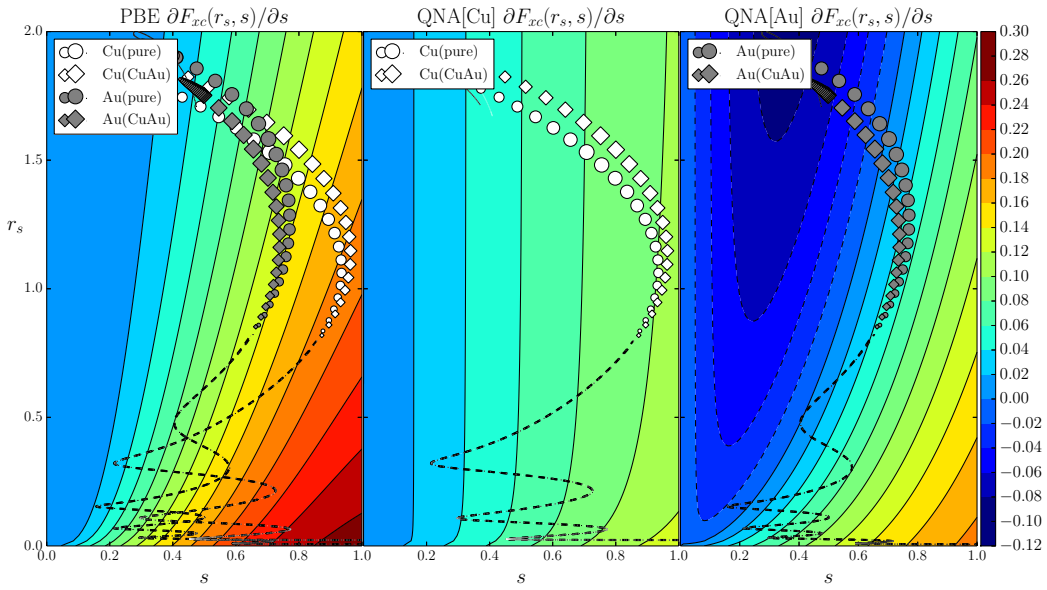

FIG. 2. (Color online) Enhancement function maps $[\partial F_{xc}(r_s,s)/\partial s]$ for PBE, QNA[Cu], and QNA[Au]. s vs. r_s curves are drawn for pure elements and for elements in the CuAu alloy. Parts of the curves drawn using symbols represent the core-valence overlap region and the size of the symbols indicate the magnitude of change between the pure element curve and the alloy component curve. Regions outside the relevant core-valence overlap region are drawn using dashed lines.

agreement with experiment. Hence, the superior performance of QNA must have a more profound reason than the trivial "volume effect".

To probe the origin of the semilocal formation energy problem, we define an "XC formation energy" (in units of meV/atom) as

$$\Delta H^{\rm xc} = \Delta H^{\rm total} - \Delta H^{\rm other}, \qquad (1)$$

where $\Delta H^{\rm total}$ is the usual formation energy and $\Delta H^{\rm other}$ includes contributions to the formation energy coming from the kinetic energy, external potential, and Hartree potential. Within a semilocal XC scheme, $\Delta H^{\rm xc}$ can be further broken down to contributions of each alloy constituent defined within the particular Wigner-Seitz cells. Accordingly, for Cu_nAu_m $\Delta H^{\rm xc}$ may be decomposed as

$$\Delta H^{\rm xc} = \frac{n\Delta H^{\rm xc}[{\rm Cu}] + m\Delta H^{\rm xc}[{\rm Au}]}{n+m}. \qquad (2)$$

Drastic differences are expected in the above defined, component resolved XC formation energies $\Delta H^{\rm xc}$[Cu/Au] calculated for different functionals. This is indeed the case, as illustrated in Table I for the case of Cu_3Au. In these test calculations, $V_{\rm QNA}$ of Cu_3Au was used for all three XC functionals. As mentioned earlier, this approximation does not alter significantly the predicted formation energies. Since all three total energies were evaluated from the LDA charge density, the $\Delta H^{\rm other}$ term in (1) remains constant (18 meV/atom) and hence its effect on the results can be factored out.

TABLE I. Alloy component resolved exchange-correlation formation energies (meV/atom) for Cu_3Au calculated at LDA, PBE and QNA levels.

Cu_3Au	$\Delta H^{\rm xc}$[Cu]	$\Delta H^{\rm xc}$[Au]	$\Delta H^{\rm xc}$	$\Delta H^{\rm other}$	$\Delta H^{\rm total}$
LDA	−1574	4468	−64	18	−46
PBE	−1623	4617	−63	18	−46
QNA	−1612	4490	−87	18	−69

QNA, which produces an accurate formation energy for Cu_3Au, clearly has the lowest $\Delta H^{\rm xc}$. For both LDA and PBE, $\Delta H^{\rm xc}$ is significantly more positive, leading to highly underestimated formation energies (in absolute value). Apparently, LDA and PBE fail for different reasons. While $\Delta H^{\rm xc}$[Cu] are very similar for PBE and QNA, PBE greatly overestimates $\Delta H^{\rm xc}$[Au] compared to QNA. Conversely, $\Delta H^{\rm xc}$[Au] of LDA and QNA are close to each other, but $\Delta H^{\rm xc}$[Cu] of LDA is considerably smaller in absolute value than the QNA one.

Most interestingly, the above findings are consistent with the trends obtained for the equilibrium volumes [18, 23]: the LDA volume for Au is accurate, while PBE strongly overestimates it. Additionally, the PBE volume for Cu is acceptable, while LDA greatly underestimates it. This observation suggests that accurate formation energies for Cu-Au require XC functionals which are suitable for both alloy constituents. Within the semilocal GGA functionals, QNA is designed to meet this strict demand.

We can shed further light on the physics of formation

TABLE II. Formation energies (meV/atom) of selected binary alloys calculated at LDA, PBE, QNA, SCAN, and HSE (Ref. [9]) levels. Available low-temperature experimental data are listed for reference. The structures are listed in parenthesis. The disordered AgPd was modeled by a 32-atom fcc special quasi-random structure. The best semilocal results are in boldface (for CuAg w.r.t HSE). The last column reports the the mean absolute relative error (MARE). SCAN and PBE(Aims) result are calculated with FHI-aims program [34–36].

	Cu_3Au ($L1_2$)	CuAu ($L1_0$)	$CuAu_3$ ($L1_2$)	CuPd ($B2$)	CuAg ($L1_0$)	CuPt ($L1_1$)	AgPd (fcc)	AgAu ($L1_0$)	NiAl ($B2$)	MARE (in %)
LDA	−39	−54	−18	−138	103	−119	−39	−64	−731	36
PBE	−45	−57	−24	−143	93	−145	−42	−59	**−678**	30
PBE(Aims)	−38	−47	−20	−120	103	**−154**	−46	−60	−655	38
QNA	**−70**	**−87**	**−41**	**−141**	**76**	**−154**	**−27**	**−46**	−689	**7**
SCAN	−64	−78	**−37**	−126	124	**−193**	−56	−83	−783	36
HSE	−71	−91	−53	−170	74	...	...	−52	...	...
Experiment	−74[9]	−93[9]	−39[9]	-140 ± 21 [9]	...	−174[40]	-23 ± 3[41]	−48[39]	−680[42]	...

energies by studying the alloying-induced changes in the electronic structure in conjunction with the explicit form of the XC formation energy $\Delta H^{\rm xc} = \Delta \int h^{\rm xc}(\mathbf{r})d\mathbf{r}$ with $h^{\rm xc} \equiv \epsilon_{\rm x}^{\rm LDA}(r_s)F_{\rm xc}(r_s,s)$. Here $\epsilon_{\rm x}^{\rm LDA}(r_s)$ is the LDA exchange energy density, $F_{\rm xc}(r_s,s)$ the enhancement function, $r_s = [3/(4\pi n)]^{1/3}$ the electronic Wigner-Seitz radius, $s = |\nabla n|/[2(3\pi^2)^{1/3}n^{4/3}]$ the reduced density gradient and n the electron density. The semilocal nature of GGA is incorporated through the s dependence of $F_{\rm xc}(r_s,s)$. With the above forms, the change in the alloy component resolved XC formation energy density reads

$$\Delta h^{\rm xc} = \frac{d\epsilon_{\rm x}^{\rm LDA}(r_s)}{dr_s}F_{\rm xc}(r_s,s)\Delta r_s + \\ + \epsilon_{\rm x}^{\rm LDA}(r_s)\left[\frac{\partial F_{\rm xc}(r_s,s)}{\partial r_s}\Delta r_s + \frac{\partial F_{\rm xc}(r_s,s)}{\partial s}\Delta s\right], \quad (3)$$

where Δr_s and Δs stand for the changes in r_s and s upon alloying. Since these changes are computed from the LDA densities, they remain the same for all semilocal functionals, and thus the differences between the three $\Delta H^{\rm xc}$[Cu/Au] values in Table I should be associated with the enhancement factors. Actually, the first two terms in (3) are very similar for the three functionals, which places the $\partial F_{\rm xc}/\partial s$ term in spotlight. The maps of $\partial F_{\rm xc}^{\rm PBE}/\partial s$, $\partial F_{\rm xc}^{\rm QNA[Au]}/\partial s$ and $\partial F_{\rm xc}^{\rm QNA[Cu]}/\partial s$ are shown in Figure 2 as a function of r_s and s. In this figure, we also plot the actual spherically averaged (r_s,s) values for Cu and Au in Cu_3Au alloy and in pure Cu and Au. Symbols mark the so called core-valence overlap region (CVOR), and the sizes of the symbols are chosen proportional to the strength of the changes. It is important to notice that the changes in Δr_s and Δs and thus the physically relevant area for $\Delta H^{\rm xc}$ are located in the highlighted CVOR. Many previous studies [24, 25, 43–45] have reached similar conclusions regarding the importance of the CVOR for the equilibrium volume.

Within the CVOR[Cu], $\Delta s > 0$ and $\partial F_{\rm xc}^{\rm QNA[Cu]}/\partial s \simeq \partial F_{\rm xc}^{\rm PBE}/\partial s > 0$ so that $\Delta H_{\rm PBE}^{\rm xc}$[Cu] $\simeq \Delta H_{\rm QNA}^{\rm xc}$[Cu] $< \Delta H_{\rm LDA}^{\rm xc}$[Cu]. On the other hand, within the CVOR[Au], $\Delta s < 0$ and $\partial F_{\rm xc}^{\rm PBE}/\partial s > \partial F_{\rm xc}^{\rm QNA[Au]}/\partial s \simeq 0$ and thus $\Delta H_{\rm PBE}^{\rm xc}$[Au] $> \Delta H_{\rm QNA}^{\rm xc}$[Au] $\approx \Delta H_{\rm LDA}^{\rm xc}$[Au]. These estimated trends of the XC formation energies fully explain the numbers in Table I. We can conclude that this particular feature of the PBE map around the CVOR [Au], specifically the large $\partial F_{\rm xc}^{\rm PBE}/\partial s$, is catastrophic for Au and leads to heavily overestimated $\Delta H^{\rm xc}$[Au].

Actually, the interplay between the shape of the $\partial F_{\rm xc}/\partial s$ maps and the (system dependent) (r_s,s) curves can elucidate the performance of the functionals for the equilibrium volume as well. Haas *et al.* [25] demonstrated how the volume (Ω) derivative of the XC energy ($E_{\rm xc}$) determines the equilibrium volume: larger $\partial E_{\rm xc}/\partial\Omega$ generally corresponds to smaller volume and vice versa. Since $\partial F_{\rm xc}^{\rm GGA}/\partial s$ gives a negative contribution to $\partial E_{\rm xc}/\partial\Omega$ (volume expansion means $\Delta s > 0$), an increased $\partial F_{\rm xc}^{\rm GGA}/\partial s$ results in a larger volume. In the present case, the particularly large $\partial F_{\rm xc}^{\rm PBE}/\partial s$ explains the large PBE equilibrium volume obtained for Au. In contrast, the nearly vanishing (or slightly negative) $\partial F_{\rm xc}^{\rm QNA[Au]}/\partial s$ yields a large $\partial E_{\rm xc}/\partial\Omega$ and thus smaller volume for Au as compared to PBE.

Next we demonstrate the robustness and universality of our QNA-SFA scheme with various other binary alloy systems in Table II. QNA, which handles both alloy components "correctly", turns out to give a substantial improvement over the "classical" approximations. SCAN, which has been shown to uniquely yield accurate formation energies across all MnO_2 polymorphs [8], performs well for the Cu-Au system and CuPt, but seems to overestimate CuAg, AgPd, AgAu, and NiAl.

The present results confirm that conventional LDA and GGA functionals have low accuracy in describing the energies of ordered Cu-Au system, a fact which has been found earlier by Zhang *et al.* [9] and Ozoliņš *et al.* [39]. Here we show that the accuracy of SFA-QNA for lattice constants and formation energies is superior to those

of PBE/LDA. In the case of QNA, we identify the main cause for this to be connected with the fact that QNA was designed to describe lattice constants accurately, simultaneously for all alloy components. The increased accuracy in volume ensures a better description of other quantities as well, such as the formation energy. Nevertheless, merely the "volume effect" (*i.e.* using the experimental volumes) by itself cannot account for the improved theoretical trends.

We have shown that semilocal DFT within the SFA framework is capable of accurately describing the formation energies of metallic binary alloys, previously thought to be beyond the realm of semilocal DFT. The semilocal approach presented here will have a great impact on future high-throughput projects, where more accurate results can be obtained without having to invoke higher, and often computationally more demanding, levels of DFT, such as nonlocal exchange.

The authors acknowledge the Swedish Research Council, the Swedish Foundation for Strategic Research, the Swedish Foundation for International Cooperation in Research and Higher Education, the Hungarian Scientific Research Fund (OTKA 84078 and 109570), and the China Scholarship Council for financial support. The computer resources of CSC – IT Center for Science, Finland are acknowledged.

[1] R. M. Dreizler and E. K. U. Gross, *Density Functional Theory* (Springer-Verlag, Berlin, 1990).
[2] J. P. Perdew and K. Schmidt, Density Functional Theory and its Application to Materials **577**, 1 (2001).
[3] Y. Zhao and D. G. Truhlar, J Chem Phys **125**, 194101 (2006).
[4] Y. Zhao and D. G. Truhlar, Journal of Physical Chemistry a **110**, 13126 (2006).
[5] Y. Zhao and D. G. Truhlar, Theoretical Chemistry Accounts **120**, 215 (2008).
[6] J. Sun, R. Haunschild, B. Xiao, I. W. Bulik, G. E. Scuseria, and J. P. Perdew, J Chem Phys **138**, 044113 (2013).
[7] J. Sun, A. Ruzsinszky, and J. P. Perdew, Phys. Rev. Lett. **115**, 036402 (2015).
[8] D. A. Kitchaev, H. Peng, Y. Liu, J. Sun, J. P. Perdew, and G. Ceder, Phys. Rev. B **93**, 045132 (2016).
[9] Y. Zhang, G. Kresse, and C. Wolverton, Phys. Rev. Lett. **112**, 075502 (2014).
[10] J. Heyd, G. E. Scuseria, and M. Ernzerhof, J. Chem. Phys. **118**, 8207 (2003).
[11] J. Heyd, G. E. Scuseria, and M. Ernzerhof, J. Chem. Phys. **124**, 219906 (2006).
[12] J. P. Perdew, K. Burke, and M. Ernzerhof, Phys. Rev. Lett. **77**, 3865 (1996).
[13] J. P. Perdew, A. Ruzsinszky, G. I. Csonka, O. A. Vydrov, G. E. Scuseria, L. A. Constantin, X. Zhou, and K. Burke, Phys. Rev. Lett. **100**, 136406 (2008).
[14] R. Armiento and A. E. Mattsson, Phys. Rev. B **72**, 085108 (2005).
[15] W. Kohn and A. E. Mattsson, Phys. Rev. Lett. **81**, 3487 (1998).
[16] R. Armiento and A. E. Mattsson, Phys. Rev. B **66**, 165117 (2002).
[17] H. Levämäki, M. P. J. Punkkinen, K. Kokko, and L. Vitos, Phys. Rev. B **86**, 201104 (2012).
[18] H. Levämäki, M. P. J. Punkkinen, K. Kokko, and L. Vitos, Phys. Rev. B **89**, 115107 (2014).
[19] L. Vitos, H. L. Skriver, B. Johansson, and J. Kollár, Comput. Mater. Sci. **18**, 20 (2000).
[20] L. Vitos, Phys. Rev. B **64**, 014107 (2001).
[21] L. Vitos, I. A. Abrikosov, and B. Johansson, Phys. Rev. Lett. **87**, 156401 (2001).
[22] L. Vitos, *Computational Quantum Mechanics for Materials Engineers: EMTO Method and Applications* (Springer: London, 2007).
[23] M. Ropo, K. Kokko, and L. Vitos, Phys. Rev. B **77**, 195445 (2008).
[24] G. I. Csonka, J. P. Perdew, A. Ruzsinszky, P. H. T. Philipsen, S. Lebegue, J. Paier, O. A. Vydrov, and J. G. Angyan, Phys. Rev. B **79**, 155107 (2009).
[25] P. Haas, F. Tran, P. Blaha, K. Schwarz, and R. Laskowski, Phys. Rev. B **80**, 195109 (2009).
[26] R. Orr, Acta Metallurgica **8**, 489 (1960).
[27] H. Okamoto, D. Chakrabarti, D. Laughlin, and T. Massalski, J. Phase Equilibria **8**, 454 (1987).
[28] P. Villars, ASM International Materials Park, OH (2006).
[29] M. Sanati, L. G. Wang, and A. Zunger, Phys. Rev. Lett. **90**, 045502 (2003).
[30] S.-H. Wei, A. A. Mbaye, L. G. Ferreira, and A. Zunger, Phys. Rev. B **36**, 4163 (1987).
[31] K. Terakura, T. Oguchi, T. Mohri, and K. Watanabe, Phys. Rev. B **35**, 2169 (1987).
[32] A. V. Ruban, I. A. Abrikosov, and H. L. Skriver, Phys. Rev. B **51**, 12958 (1995).
[33] S. L. Shang, A. Saengdeejing, Z. G. Mei, D. E. Kim, H. Zhang, S. Ganeshan, Y. Wang, and Z. K. Liu, Comput. Mater. Sci. **48**, 813 (2010).
[34] V. Blum, R. Gehrke, F. Hanke, P. Havu, V. Havu, X. Ren, K. Reuter, and M. Scheffler, Computer Physics Communications **180**, 2175 (2009).
[35] V. Havu, V. Blum, P. Havu, and M. Scheffler, Journal of Computational Physics **228**, 8367 (2009).
[36] FHI-aims employs numberical atomi-centered orbital basis set. Tier 2 level basis set with 'tight' integration grid and 1688 (1099 for AgPd sqs system) k-point in the irreducible Brillloun zone were used. SCAN energies were evaluated non-selfconsistently using converged PBE densities. Tests show that difference between self-consistent and non-selfconsistent SCAN formation energies are small.
[37] P. Haas, F. Tran, and P. Blaha, Phys. Rev. B **79**, 085104 (2009).
[38] V. N. Staroverov, G. E. Scuseria, J. Tao, and J. P. Perdew, Phys. Rev. B **69**, 075102 (2004).
[39] V. Ozoliņš, C. Wolverton, and A. Zunger, Phys. Rev. B **57**, 6427 (1998).
[40] Z. W. Lu, S. H. Wei, A. Zunger, S. Frota-Pessoa, and L. G. Ferreira, Phys. Rev. B **44**, 512 (1991).
[41] D. Feng and P. Taskinen, J. Mater. Sci. **49**, 5790 (2014).
[42] R. E. Watson and M. Weinert, Phys. Rev. B **58**, 5981 (1998).
[43] M. Fuchs, M. Bockstedte, E. Pehlke, and M. Scheffler, Physical Review B **57**, 2134 (1998).

[44] A. Zupan, P. Blaha, K. Schwarz, and J. P. Perdew, Physical Review B **58**, 11266 (1998).

[45] A. V. Ruban and I. A. Abrikosov, Reports on Progress in Physics **71**, 046501 (2008).